

Spectral anisotropy and intermittency of plasma turbulence at ion kinetic scales

Simone Landi

*Dipartimento di Fisica e Astronomia, Università di Firenze, Firenze, Italy. and
Osservatorio Astrofisico di Arcetri, INAF, Firenze, Italy*

Luca Franci

School of Physics and Astronomy, Queen Mary University of London, London, UK

Emanuele Papini and Andrea Verdini

Dipartimento di Fisica e Astronomia, Università di Firenze, Firenze, Italy.

Lorenzo Matteini

*LESIA, Observatoire de Paris,
Université PSL, CNRS, Sorbonne Université,
Univ. Paris-Diderot, Sorbonne Paris Cité
place J. Janssen 5, F-92192 Meudon, France**

Petr Hellinger

*Astronomical Institute, CAS, Bocni II/1401, CZ-14100 Prague, Czech Republic and
Institute of Atmospheric Physics, CAS, Bocni II/1401, CZ-14100 Prague, Czech Republic*

(Dated: April 18, 2019)

By means of three dimensional high-resolution hybrid simulations we study the properties of the magnetic field spectral anisotropy near and beyond ion kinetic scales. By using both a Fourier analysis and a local analysis based on multi-point 2nd-order structure function techniques, we show that the observed anisotropy is less than what expected by standard wave normal modes turbulence theories although the non linear energy transfer is still in the perpendicular direction with respect to the magnetic field, only advected in the parallel direction as expected balancing the non-linear energy transfer time and the decorrelation time. Such result can be explained by a phenomenological model based on the formation of strong intermittent two-dimensional structures in the plane perpendicular to the local mean field that fulfill some prescribed aspect ratio eventually depending on the scale. This model supports the idea that small scales structures, such as reconnecting current sheets, contribute significantly to the formation of the turbulent cascade at kinetic scales.

I. INTRODUCTION

The solar wind plasma is coupled to electromagnetic fluctuations whose spectra follow power laws spanning a huge range of frequencies and are the signature of a strong turbulent activity that taking place in there [e.g. 1–3]. At 1 AU, plasma fluctuations with frequencies in the interval $10^{-4} \text{ Hz} \lesssim f \lesssim 10^{-2} \text{ Hz}$ are reasonably well described by the one-fluid magneto-hydrodynamic (MHD) equations: there, the spectra of the magnetic field, the ion bulk velocity, and the electric field are dominated by the transverse components with respect to the ambient magnetic field \mathbf{B}_0 . Magnetic fluctuations typically show a Kolmogorov-like spectrum (i.e., having the $-5/3$ slope), while the velocity field power is slightly shallower (typically close to $-3/2$) [e. g. 4–8] and strongly coupled with electric field fluctuations [9] as expected in the ideal MHD regime. This regime is the so-called MHD inertial range.

At higher frequencies, $f \gtrsim 10^{-1} \text{ Hz}$, corresponding to length scales approaching typical ion kinetic scales, there is a change in the properties of the observed fluctuations. Near these scales, a spectral transition (break) appears in the magnetic field fluctuations, separating the MHD inertial range

from a second, steeper, power-law interval at kinetic scales. There is a certain degree of variability of the spectral index just below this transition [e. g. 10–12], although the slope seems more universal at higher frequencies with an index of -2.8 [13, 14]. At those scales, the ion bulk velocity decouples from magnetic field fluctuations and its spectrum shows (if any) an even steeper power-law slope [e.g. 15]; on the contrary, the electric field spectrum is shallower at sub-ion scales [16, 17] and becomes dominant over the magnetic field power, with a typical spectral index around -0.8 [e.g. 18, 19], consistent with the scaling predicted by the generalized Ohm's law [20]. Which ion characteristic kinetic scale is the most relevant in determining the position of such transition has not been clearly identified, although observational evidences [21, 22] and numerical simulations [23] suggest that it is likely related to the larger between the ion inertial length and the ion gyroradius for extreme values of the the plasma beta, and to a combination of both in the intermediate-beta regime. At ion kinetic scales, also the nature of the fluctuations changes: an increase of the magnetic compressibility [24, 25] and a reduced variance anisotropy [26] are observed; the density, while it follows a Kolmogorov spectrum at MHD scales, shows a flattening near the break [27], then becomes strongly coupled to the magnetic field fluctuations at sub-ion scales [28].

An important aspect of plasma turbulence is how the cas-

* Department of Physics, Imperial College London, London SW7 2AZ, UK.

cade toward small scales proceeds with respect to the parallel and perpendicular component of a large scale mean magnetic field. At fluid scales, three-dimensional (3D) numerical simulations [e. g. 29–40] have highlighted the role of spectral anisotropy in the formation of the MHD turbulent spectra, including the case when the radial expansion of the solar wind is taken into account [41–43]. In particular several numerical simulations [e.g. 31, 32, 44] have shown that spectra tend to organize themselves in the so called critical balance state [45–47], in which the cascade proceeds by transferring energy only to scales where the non-linear interactions of eddies are faster than the linear propagating time of the normal modes of the fluid system. At such scales, this balance predicts that energy is transferred mostly in the direction perpendicular to the (local) mean field following a Kolmogorov cascade, while the parallel spectrum should decrease as k_{\parallel}^{-2} . As a consequence, the two-dimensional (2D) spectral anisotropy should scale as $k_{\parallel} \propto k_{\perp}^{2/3}$ [30, 48]. Observations seem to confirm to some extent that such energy transfer occurs in the solar wind plasma [7, 49–53].

The critical balance argument can be extended to the kinetic (sub-ion) scales, provided that one uses the electron-velocity eddy turn-over time as the relevant non-linear time and takes into account the dispersive nature of the fluctuations in this regime. Regardless of the normal mode used, either low-frequency strongly-oblique propagating Kinetic Alfvén Waves (KAW) [54] or quasi-parallel high-frequency whistler modes [55], standard wave-wave interaction models of turbulence predict for the magnetic field spectrum a $k_{\perp}^{-7/3}$ scaling at sub-ion scales, and a further increase of the spectral anisotropy $k_{\parallel} \propto k_{\perp}^{1/3}$ with a steeper (than MHD scales) parallel spectrum $\propto k_{\parallel}^{-5}$. A magnetic power decreasing as $k^{-7/3}$ has indeed been observed in several simulations using electron MHD [e. g. 55–59], Hall MHD [60] and gyrokinetic models [61]. Numerical evidence of the critically balanced scaling $k_{\parallel} \propto k_{\perp}^{1/3}$ have been reported by Cho and Lazarian [58].

Steeper magnetic field spectra, $\propto k_{\perp}^{-2.8}$, in good agreement with solar wind observations, have been reproduced in gyrokinetic simulations [62] where the steepening (with respect to the $-7/3$ prediction) was attributed to electron Landau damping. Using a frequency analysis TenBarge and Howes [63] found that these simulations are in agreement with a $k_{\parallel} \propto k_{\perp}^{1/3}$ anisotropy scaling, although a perpendicular spectrum steeper than $k_{\perp}^{-7/3}$ should lead to a significant stronger anisotropy. Indeed, the critical balance condition both at MHD and kinetic scales can be written as $k_{\parallel} \propto k_{\perp} b(k_{\perp})$, with $b(k_{\perp})$ being the magnetic fluctuations amplitude at the scale k_{\perp} : as the spectrum becomes steeper, $b(k_{\perp})$ steepens and the anisotropy increases. For a spectral slope of the magnetic power $P_B = b^2(k_{\perp})/k_{\perp} \propto k_{\perp}^{-2.8}$, $b(k_{\perp}) \propto k_{\perp}^{0.9}$ and the critical balance predicts $k_{\parallel} \propto k_{\perp}^{0.1}$. In this Kolmogorov-like phenomenological model only a slope $-7/3$ is consistent with the scaling $k_{\parallel} \propto k_{\perp}^{1/3}$.

Retaining the effects of linear ion and electron Landau damping, theoretical models [64] and numerical simulations [65, 66] predict a strong variability of the slope in the perpendicular spectrum together with an increase in the spectral anisotropy in the sub-ion range. Such variability is correlated

with the ratio between the non-linear energy transfer time and the propagation/damping properties of low-frequency highly-oblique electromagnetic waves (the Kinetic Alfvén waves). Some variability of the magnetic energy slope has been reported also in 2D [67] and 3D full pic simulations [68]. However Hellinger *et al.* [69], by analysing the properties of the 3rd order structure functions in 2D high resolution numerical simulations at low and moderate values of the plasma β , have shown that the sub-ion scales electromagnetic field power can be reasonably well described by an inertial (i. e. dissipative-less) Hall-MHD range. Moreover, fluid 2D Hall-MHD simulations, where kinetic damping effects are not taken into account, has been able to produce spectra steeper than $-7/3$ in remarkably good agreement with analogous hybrid kinetic simulations and observations [70].

Several 3D numerical simulations investigating sub-ion scales have highlighted the role of coherent structures and intermittency in characterizing the turbulent cascade and its dissipation [e. g. 71–73]. Boldyrev and Perez [74] have shown that, if energy is concentrated in spatially localized structures at small scales, the spectrum of magnetic fluctuations steepens following a $-8/3$ power law [see also 75], the anisotropy should follow $k_{\parallel} \propto k_{\perp}^{2/3}$, and the parallel spectrum a $-7/2$ power-law. Meyrand and Galtier [76], in the framework of EMHD, reported a similar perpendicular scaling but a steeper parallel spectrum, $\propto k_{\parallel}^{-5}$, consistent with a turbulent cascade driven merely by a 2D dynamics. More recently, [77] reported 3D hybrid Vlasov simulations where parallel and perpendicular spectra are qualitatively consistent with the model proposed by [74] at $\beta_p = 1$ while steeper slopes are observed for a lower value of the proton plasma beta ($\beta_p = 0.2$). Concurrently, Franci *et al.* [78], by analyzing the spectral properties of a high-resolution hybrid PIC simulation able to cover almost two decades in k -vectors, found that the spectral anisotropy, though large in the inertial range, becomes frozen in the sub-ion range following a $k_{\parallel} \propto k_{\perp}$ scaling. A similar observation have been reported by Arzamasskiy *et al.* [79].

In this work we present results from a high-resolution Particle-in-cell (PIC) hybrid (fluid electrons, kinetics protons) 3D numerical simulation of freely-decaying turbulence in presence of a mean magnetic field. This simulation is very similar to that described in Franci *et al.* [78], but uses a very high spatial grid resolution to focus on the spectral anisotropies at sub-ion scales. Fourier spectra show a transition near the ion scales and the simulation is able to produce a well defined spectrum in the kinetic range over more than one decade. A closer inspection of the magnetic and the density spectra shows that the spectral anisotropy with respect to the mean field stops to increase near the ion scales but the turbulent cascade still proceeds essentially in the perpendicular direction. A local analysis, using the multi-point 2nd-order structure function technique confirms that the anisotropy is frozen also with respect to the local mean field. Such result can be interpreted by generalizing the model proposed by [74] and assuming that, at ion scales, the energy is mostly contained in intermittent coherent structures whose characteristic filling factor follows a prescribed scaling. This seems to

be consistent with models [80–83] and numerical simulations [84, 85] which show that current sheets actively participate in the formation of the turbulent cascade.

II. NUMERICAL SETUP

We employ the hybrid particle-in-cell (HPIC) code CAMELIA (Current Advance Method Et cycLIc leApfrog) [86], where the electrons are considered as a massless, charge neutralizing fluid, whereas the ions (protons) are described by a particle-in-cell model (see Matthews [87] for detailed model equations) and are advanced by the Boris scheme. Units of mass, length, and time are the ion (proton) mass m_i , its inertial length d_i and the inverse of its gyroradius $1/\Omega_i$. We use 512^3 collocation points in a spatial cubic grid with resolution $\Delta x = \Delta y = \Delta z = 0.0625 d_i$ and 2048 particles per cell (ppc) representing ions. Accumulation of energy at small scales is prevented by adopting a resistivity coefficient $\eta = 1.5 \times 10^{-3} 4\pi v_A c^{-1} \Omega_i^{-1}$. The ions are advanced with a time step $\Delta t = 0.00625 \Omega_i^{-1}$, while the magnetic field \mathbf{B} is advanced with a smaller time step $\Delta t_B = \Delta t/10$. The initial condition consists of a uniform and neutral plasma density $n = n_i = n_e$, a uniform magnetic field directed along z , $\mathbf{B}_0 = B_0 \hat{z}$, where species have isotropic and equal temperatures, $T_i = T_e$. The relative strength of the thermal and field pressure is measured in term of the ion (electron) plasma beta, $\beta_{i,e} = 8\pi n K_B T_{i,e} / B_0^2$, K_B being the Boltzmann's constant. The setup of the simulation is similar to that shown in [78]: Decorrelated, Alfvénic-like fluctuations, initially isotropic in the 3D k -space vector range $0.20 < kd_i < 0.80$, perturb the initial condition and are left to decay. The energy is equally partitioned between velocity and magnetic field with $B^{\text{rms}}/B_0 \sim 0.38$, the electron and proton temperatures are the same $\beta_e = \beta_i = 0.5$. The analysis here reported has been performed at the maximum of the turbulent activity, $t = t_{\text{max}} \equiv 36 \Omega_i^{-1}$, when the current density rms reaches its peak [78]. The maximum of turbulent activity time here is less than the simulation shown in Franci *et al.* [78], simply because the energy is initially injected at smaller scales. Anyway, rms and physical quantities evolve in a very similar manner.

III. RESULTS

An overview of the spectral properties of the simulation is shown in Fig. (1) where we report the magnetic (top) and density (middle) omnidirectional (i. e., integrating the 3D power spectrum over all the possible directions) power spectra as a function of the perpendicular (solid) and parallel (dashed) k -vectors

$$P_{1D}(k) = \int_0^{2\pi} \int_{-1}^1 k^2 P(k \cos \phi \cos \theta, k \sin \phi \cos \theta, k \sin \theta) d\phi d(\cos \theta). \quad (1)$$

The original spectra, shown as dotted lines in each panel, are obtained by removing the numerical noise accumulated at small scales, in a way similar to that shown in [78]: we set

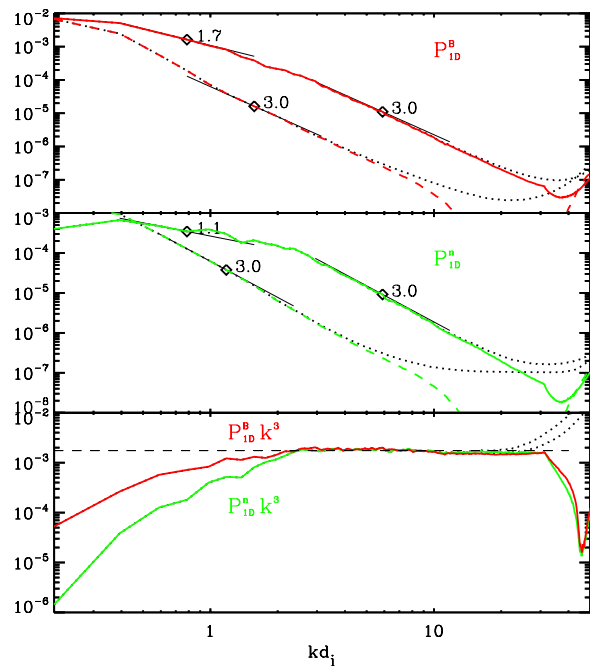


FIG. 1. 1D reduced perpendicular (solid) and parallel (dashed) spectra of magnetic (top panel) and density fluctuations (middle). Power laws are drawn in thin solid black lines as a reference. On the bottom the isotropized 1D spectra of B (red) and density n (green) compensated by k^3 . The spectra are obtained by applying a post-processing filtering procedure (see text for details). The unfiltered spectra are shown as dotted black curves.

to zero the amplitude of each 3D Fourier mode whose wave-number modulus is larger than a defined cut-off k_{cf} . Moreover, we set to zero also all the modes of all the fields for which the magnetic energy density is less than a given noise threshold. Here the noise level has been chosen as 10^{-11} and the cut-off is $k_{cf} = 2k_{\text{max}}/3 \approx 170k_0$ with $k_0 = 2\pi/L_x$ and k_{max} the Nyquist wave-vector. For both fields, the reduced spectra in the perpendicular direction show a well defined -3 power law over almost one-decade for $kd_i > 1$. At large scales the filtered and unfiltered spectra are superimposed while the filtering procedure allows to extend the power-law in the high k -vector region. As expected, for both fields, at all scales the parallel reduced spectrum is subdominant with respect to its perpendicular counterpart, meaning that a spectral anisotropy is developed; however its power-law slope is the same as the perpendicular reduced spectrum, meaning that the spectral anisotropy produced at large scales $k_{\perp} d_i < 1$ is then frozen at sub-ion scales $k_{\perp} d_i > 1$.

To understand the reduced 1D power spectra it is useful to analyse the reduced 2D spectra obtained by integrating the 3D spectra over all possible directions in the plane perpendicular to the main field.

$$P_{2D}(k_{\parallel}, k_{\perp}) = \int_0^{2\pi} k_{\perp} P(k_{\perp} \cos \phi, k_{\perp} \sin \phi, k_{\parallel}) d\phi. \quad (2)$$

In Fig. 2, the 2D reduced spectrum of the magnetic fluctu-

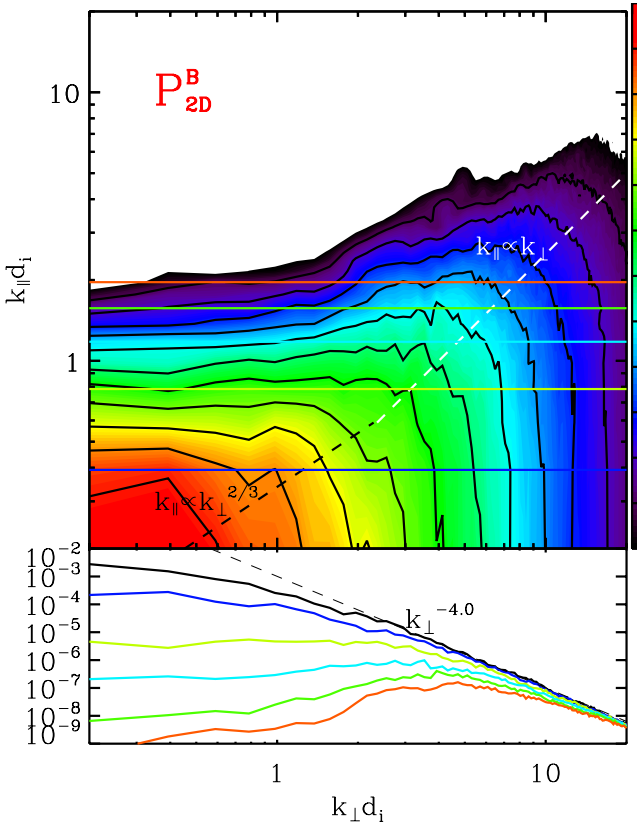


FIG. 2. Top panel: Reduced 2D spectrum of the total magnetic field fluctuations in the $(k_{\perp}, k_{\parallel})$ space (log-log scale) at $t = 36\Omega_i^{-1}$. The dashed white line highlights the $k_{\parallel} \propto k_{\perp}$ scaling in the $2 \leq k_{\perp} \leq 20$ region. A $k_{\parallel} \propto k_{\perp}^{2/3}$ (dashed black line) in the low k_{\perp} domain is also included as reference. Bottom panel: Cuts of the 2D spectrum for $k_{\parallel} = \text{const}$: each color corresponds to a cut in k_{\parallel} outlined with the same color in the top panel (the black line corresponds to $k_{\parallel} = 0$).

ations in log-log scale is shown. At large scales a spectral anisotropy is developed with the power mostly confined in the region $k_{\perp} > k_{\parallel}$. At higher wave-vectors, $k_{\perp} d_i \gtrsim 1$, this anisotropy appears to remain almost constant and most of the power seems confined in a region $k_{\parallel} \propto k_{\perp}$ (highlighted with the dashed white-line here used only as reference). Such a behaviour is different from the spectral anisotropy predicted by the critical balance conditions in KAW or Whistler mediated turbulence ($k_{\parallel} \propto k_{\perp}^{1/3}$) [54, 58] and also to that proposed by [74] where a spectral anisotropy $k_{\parallel} \propto k_{\perp}^{2/3}$ was obtained taking also into account the effect of the intermittency. A closer inspection to the 2D spectrum shows that in the region where the spectral anisotropy is frozen (constant aspect ratio) the iso-levels are almost independent of k_{\parallel} meaning that the energy transfer occurs essentially in the perpendicular direction. To better elucidate this, cuts with $k_{\parallel} = \text{const}$ of the 2D reduced spectra are shown in the bottom panel of Fig. 2. For small value of k_{\parallel} , they have a significant level of energy at small value of k_{\perp} and with different slopes. On the other hand, at approximately $k_{\perp} d_i = 2$ they all collapse and

follow the same power-law which is well approximated by $P_{2D}^B(k_{\perp}, k_{\parallel} = \text{const}) \propto k_{\perp}^{-4}$. Cuts with larger values of k_{\parallel} are almost depleted of energy for small values of k_{\perp} which then increases near $k_{\perp} = Ck_{\parallel}$, following approximately the same power law, $\propto k_{\perp}^{-4}$ (until small-scale numerical effects become dominant).

At the lowest level of approximation, the 2D magnetic power spectrum at small scales can be described as a spectrum that is almost independent on k_{\parallel} and bounded by the condition $k_{\perp} \leq Ck_{\parallel}^{\alpha}$ and where each perpendicular spectrum at constant k_{\parallel} follows a $k_{\perp}^{-\beta}$ power-law:

$$\begin{cases} P_{2D}^B = P_0 k_{\perp}^{-\beta} & \text{if } |k_{\parallel}| < k_{\perp}^{\alpha} \\ 0 & \text{Otherwise} \end{cases} \quad (3)$$

Such simplified 2D model produces a reduced perpendicular spectrum $k_{\perp}^{\alpha-\beta}$, while the parallel one goes as $k_{\parallel}^{(1-\beta)/\alpha}$. If we now assume $\alpha = 1$ and $\beta = 4$ we obtain the same power-law -3 for both perpendicular and parallel spectra. Within this model one should observe $\beta = 10/3$ if the spectral anisotropy was the one proposed by [74] ($\alpha = 2/3$) while $\beta = 6/3$ is the power-law required to obtained the reduced spectra in the self-similar model of turbulence ($\alpha = 1/3$). Both values are significantly shallower than the behavior observed in our simulation.

One important question that arises here is whether the z -direction maps correctly the parallel direction of the (local) mean field, that is, the relevant framework with respect to which the spectral anisotropy properties are supposed to be valid [7, 30, 48, 50, 58, 88]. To this aim, the scale-dependent anisotropy can be measured using the 2nd order structure function (SF_2) calculated in the local frame. However, since the slope of the fluctuations is near -3 in the sub-ion range, the usual 2-points 2nd-order structure function is not suitable to study the spectral anisotropy at such scales and multi-points 2nd-order structure functions must be used [88, 89]. Here we use the 3- and 5-points for a quantity A , defined respectively as

$$SF_2^{(3)}(\mathbf{r}; A) = \langle \delta A^2 \rangle = \langle (A(\mathbf{x}+\mathbf{r}) - 2A(\mathbf{x}) + A(\mathbf{x}-\mathbf{r}))^2 \rangle \quad (4)$$

and

$$SF_2^{(5)}(\mathbf{r}; A) = \langle \delta A^2 \rangle = \langle (A(\mathbf{x}+2\mathbf{r}) - 4A(\mathbf{x}+\mathbf{r}) + 6A(\mathbf{x}) - 4A(\mathbf{x}-\mathbf{r}) + A(\mathbf{x}-2\mathbf{r}))^2 \rangle \quad (5)$$

These functions are roughly proportional to r^{m-1} for a spectral slope $\propto k^{-m}$ if $m < 5$ ($SF_2^{(3)}$) and $m < 9$ ($SF_2^{(5)}$) respectively. Fig. 3 reports the structure functions for the magnetic and the density fields measured in the local frame: this is defined by the parallel to the local mean direction \mathbf{B}_L , which is the average field $\langle \mathbf{B} \rangle$, seen in the interval $(\mathbf{x}, \mathbf{x} + \mathbf{r})$ and by the fluctuations $\delta \mathbf{B}$: $\hat{l} = \mathbf{B}_L / B_L$ (dash-dotted lines) is the unit vector parallel to the local mean direction, $\hat{\lambda}$ (solid) is the unit vector normal to the both \hat{l} and to $\delta \mathbf{B}$, while $\hat{\xi} = \hat{l} \times \hat{\lambda}$ (dashed) completes the reference frame. As expected the 2nd-order structure functions are more energetic in the perpendicular component: for separations smaller than about d_i they follow approximately a power-law whose index $m - 1$ correspond to

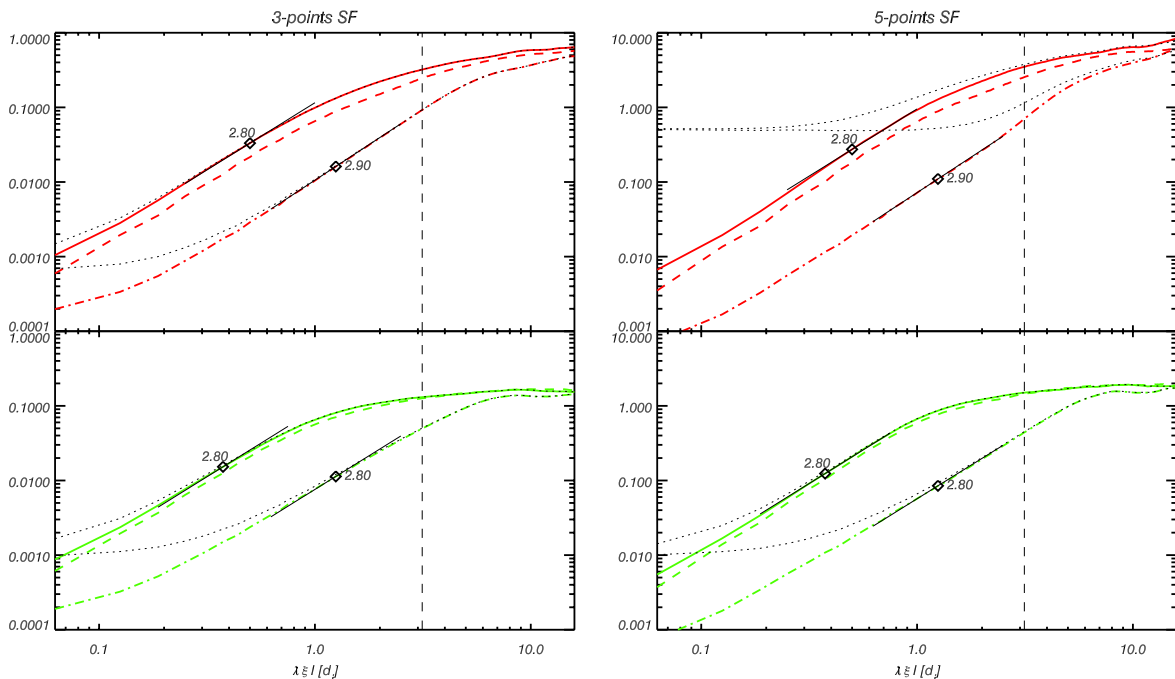


FIG. 3. Local 2nd-order 3 (left) and 5 (right) points structure functions for the magnetic (top), and density (bottom) fields. Solid and dashed lines are the two perpendicular components $\hat{\lambda}$ and $\hat{\zeta}$ while the dash-dotted is for the parallel one \hat{l} . Power laws are drawn in thin solid black lines as a reference and are expressed in terms of the corresponding slopes in Fourier spectra. Dotted lines are the same quantities computed without using the filtering procedure outlined in the text.

a spectral index $m = 2.8$, not far to what observed in Fourier spectra. The important result here is however related to the behaviour of the direction parallel to the local field, which follows the same power-law as the perpendicular counterpart, shifted roughly by a factor of five to larger scales. The results is quite robust being almost the same for both the 3-point and 5-point SFs and confirm that, in this simulation where a relatively strong mean field is present, global spectra reproduce the spectral anisotropy at local scales. It should be noticed also, that such result is consistent with Arzamasskiy *et al.* [79] in which a spectral anisotropy scaling as $k_{\parallel} \propto k_{\perp}$ with respect to the local mean field was observed in analogous hybrid kinetic simulations by using a different technique based on Fourier-space filtering.

The SFs here reported are computed using the fields recovered in the real space once the filtering procedure has been applied in Fourier space: In the same figure (dotted-lines) are also reported the SFs computed without the filtering to show the effect of the noise. Although strongly localized in Fourier space, i. e. at small scales, the noise impacts significantly the SFs over a much larger interval in the separation scales and it is stronger as the statistic used for the SFs increases. The reason lies in the noise of the high- k modes which introduces in each grid point i a fluctuations $\pm \Delta f$ in the computation of the $SF_2(f)$ of the quantity f : with N the number of sampling point the quantity f^2 is affected by a systematic noise $\propto N^2$; the SFs, which are $\propto \sum_i f^2/N$, are thus affected by a systematic noise at all scales $\propto N$. We have verified that it is indeed

the case in this simulation.

IV. DISCUSSION

Both the global analysis with Fourier spectra and the one based on 2nd-order structure functions in the local magnetic field frame show that the scaling of the spectral anisotropy is significantly less than what expected from current theories of turbulence at sub-ion scales. In particular we observe a scale independent anisotropy once the ion scales are reached. It is worth underlying that although the growth of the spectral anisotropy is reduced, the 2D Fourier spectrum of the magnetic field shows that the non-linear energy transfer happens in the perpendicular direction and is only advected along the parallel direction, thus suggesting that, like in the standard model of the critical balance [45] and in RMHD models of turbulence [90, 91], the non-linear energy transfer time-scale is bounded by the decorrelation time which turns out to be that of the linear wave-propagation time.

A possible interpretation of the results follows and extends the arguments of Boldyrev and Perez [74] based on the presence of intermittent features [92] localized in a 2D space normal to the local mean field. Following that argument, let us assume that at the perpendicular scale $\lambda \propto k_{\perp}^{-1}$, the energy density fills only a fraction λ^{α} of the space. In this case the magnetic energy density scales as $E_{\lambda} \propto b_{\lambda}^2 \lambda^{\alpha}$. Then, assuming that the energy transfer time at sub-ion scales is the non

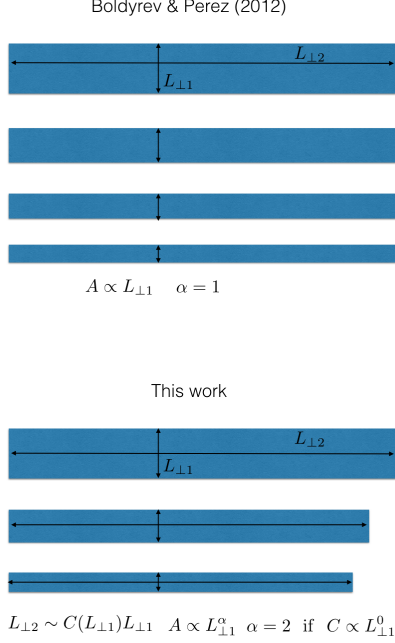


FIG. 4. Sketch of the filling factor scaling in Boldyrev and Perez [74] (top) and the generalised scaling proposed in this work (bottom).

linear time $\tau_{NL} \propto \lambda^2/b_\lambda$ [e. g. 55], and requiring that the energy flux is conserved through the scales, $E_\lambda/\tau_{NL} \propto \text{const}$, we have

$$b_\lambda \propto \lambda^{(2-\alpha)/3}, \quad (6)$$

from which

$$E_\lambda \propto \lambda^\alpha b_\lambda^2 \propto \lambda^{(4+\alpha)/3}. \quad (7)$$

Therefore the power density spectrum P_B goes as

$$P_B \propto E(k_\perp)/k_\perp \propto k_\perp^{-\frac{1}{3}(7+\alpha)}. \quad (8)$$

The requirement that the non linear time is bounded by the decorrelation time, assuming the latter given by dispersive modes [e. g., 88], requires for the parallel scale $l \propto \lambda/b_\lambda$ or $k_\parallel \propto k_\perp b(k_\perp)$ from which the spectral anisotropy is

$$k_\parallel \propto k_\perp^{\frac{1}{3}(\alpha+1)}. \quad (9)$$

In terms of the parallel scale the energy density goes as

$$E_l \propto l^{\frac{4+\alpha}{1+\alpha}} \quad (10)$$

and the power density spectrum P_B goes as

$$P_B \propto E(k_\parallel)/k_\parallel \propto k_\parallel^{-\frac{5+2\alpha}{1+\alpha}}, \quad (11)$$

For $\alpha = 0$ one recovers the standard $P_B \sim k_\perp^{-7/3}$ and $k_\parallel \propto k_\perp^{1/3}$, while taking the filling factor proportional to λ ($\alpha = 1$) Boldyrev and Perez [74] found $P_B \sim k_\perp^{-8/3}$ and a reduced anisotropy $k_\parallel \propto k_\perp^{2/3}$. Interestingly, assuming that the filling factor scales as λ^2 ($\alpha = 2$), the power given by Eq. (8) will go as k_\perp^{-3} , $B(k_\perp) \propto \text{const}$ and, following Eq. (9) the anisotropy will become scale-independent, i.e. $k_\parallel \propto k_\perp$.

A possible physical interpretation of such a result is illustrated in Fig. 4: in the plane perpendicular to the mean field, a structure has typically two characteristic lengths $l_{\perp 1}$ and $l_{\perp 2}$. In the model of Boldyrev and Perez [74] (top panel) only one characteristic length (say $l_{\perp 1}$) changes with the scale, so that the filling factor reduces linearly as $l_{\perp 1}$. However if the two characteristic lengths are correlated (for example if a specific aspect ratio of these structures is set as a function of their size) both will change with decreasing scale and the associated filling factor will be then reduced by a factor $l_{\perp 1} l_{\perp 2} \propto l_{\perp 1}^\alpha$ with $\alpha > 1$. In the special case that the aspect ratio is the same irrespective of the scale, we have $l_{\perp 2} = C l_{\perp 1}$ and $\alpha = 2$; in this case the power-law spectrum will scale as k_\perp^{-3} and the spectral anisotropy will go as $k_\parallel \propto k_\perp$ in very good agreement with our results. Note that assuming $\lambda^\alpha = \xi^\alpha$ implies $\lambda \propto \xi^{1/(\alpha-1)}$ (valid only if $\alpha \neq 1$ when the second perpendicular dimension has a meaning) from which $E_\xi \propto \xi^{(4+\alpha)/3(\alpha-1)}$. If $\alpha = 2$ also the spectrum of the second perpendicular component follows the same power-law, which is also in agreement with our simulation: however in this case it is not possible to discriminate from other models where both perpendicular components are equivalent.

V. CONCLUSION

We have analyzed the spectral anisotropy properties of plasma turbulence in a high-resolution hybrid PIC 3D simulation. The setup of the simulation is similar to that of the simulation discussed in [78] except for the higher resolution at small scales: here the grid step has been chosen 4 times smaller to better cover the sub-ion scales where our analysis is focused. The global spectral properties at sub-ion scales are very similar to what already observed: a slope steeper than $-7/3$ and $-8/3$ predicted by wave and intermittency based models, consistent with what observed in the solar wind and planetary magnetospheres and with what already observed both in 2D and 3D simulations [20, 23, 70, 77–79, 93, 94].

The main aspect investigated in this work is that in the global frame, both the parallel and perpendicular spectra show the same scaling, k^{-3} , below the ion break. This picture has been confirmed further by performing a local analysis, by means of multi-point SFs, suggesting that in the simulation the aspect ratio of the turbulent fluctuations at sub-ion scales is maintained approximately constant. We have then proposed a model, based on a generalization of the one by [74], in which the spectral slopes (and thus the spectral anisotropy) are related to the nature of the intermittent structures that populate the turbulence at small scales and how they fill the total volume.

This result is in favour of a model where intermittency

driven by 2D structures in the plane perpendicular to the main field plays a dominant role in determining the spectral properties at kinetic scales; such structures should have two characteristic lengths, both reducing with decreasing the scale, in a way that satisfies a specific aspect ratio, which can also be scale-dependent. One possibility is that the turbulent cascade is strongly mediated by magnetic reconnection events where the aspect ratio of the current sheets is the important parameter setting the efficiency of the reconnection process [e.g. 95–102]. It has been already shown in Franci *et al.* [84], Cerri and Califano [85] and Papini *et al.* [70] that the formation of a sub-ion range in 2D simulations is strongly correlated with the emergence of reconnecting events between larger scale MHD vortices. Moreover it has been shown that current sheet disruption can have consequences on the spectral properties both at MHD [81, 82, 103, 104] and kinetic scales [80, 83]. Our present findings seem to support this scenario.

Solar wind observations [e.g. 13, 105] show that the magnetic (and density) fluctuations converge toward a -2.8 scaling at smaller scales, a behaviour also well captured by high resolution 2D simulations [20, 23, 93]. In the framework of the model presented in this work, this corresponds to $\alpha = 1.4$, implying that the aspect ratio of the structure is not self-similar but depends on the scales. In this case the spectral anisotropy in the sub-ion range it is expected to moderately continue to increase as $k_{\parallel} \propto k_{\perp}^{0.8}$ and the parallel spectrum would follow a -3.25 power law.

Although measurements of the spectral anisotropy are possible in the solar wind and have been performed in the inertial range [7, 50, 51], this aspect has been more scarcely addressed at kinetic scales partly because of observational constraints. Spectral anisotropy in the sub-ion range has been discussed by Chen *et al.* [106] using Cluster measurements and using two-points 2nd-order structure functions. They found that the perpendicular spectrum was steeper than the theoretical $-7/3$, but that the spectral index in the parallel direction was less

steep than the one expected by standard wave-mediated turbulence and close to -3 . We note that these values are consistent with the predictions from our model discussed above. However, as also discussed by the authors, one should be careful in interpreting their result, since when using 2-point 2nd-order SFs the resulting spectral index is limited to -3 . Indeed, as discussed in the introduction, a slope steeper than $-7/3$ in the perpendicular spectrum, combined with the critical balance condition and without intermittency, would result in very steep parallel spectrum and large spectral anisotropies at small scales. For example a $-8/3$ scaling will give $k_{\parallel} \propto k_{\perp}^{1/6}$ and a parallel spectrum $\propto k_{\parallel}^{-11}$. In the near future, to discriminate between such models will require multi-point, multi-scale analysis space missions, as it has been proposed in the Plasma 2020 Decadal Survey [107–109].

VI. ACKNOWLEDGMENTS

We thank Tullio for stimulating discussions and Dr. Ku Fu from Tibet University to point out us useful improvements. The work has been funded by Fondazione Cassa di Risparmio di Firenze through the projects *Giovani Ricercatori Protagonisti* and the project *HYPERCRHEL*. LF was supported by the UK Science and Technology Facilities Council (STFC) grant ST/P000622/1. PH acknowledges GACR grant 15-10057S. LM was supported by the Programme National PNST of CNRS/INSU co-funded by CNES. Numerical simulations and data reduction was performed at the CINECA facilities under the programs *Accordo Quadro INAF-CINECA (2017-2019)* (grant C3A22a) and ISCRAB (grant HP10BP6XYP). This work was performed also using the Cambridge Service for Data Driven Discovery (CSD3), part of which is operated by the University of Cambridge Research Computing on behalf of the STFC DiRAC HPC Facility (www.dirac.ac.uk).

-
- [1] R. Bruno and V. Carbone, *Living Reviews in Solar Physics* **10**, 2 (2013).
- [2] K. H. Kiyani, K. T. Osman, and S. C. Chapman, *Philosophical Transactions of the Royal Society of London A: Mathematical, Physical and Engineering Sciences* **373** (2015), 10.1098/rsta.2014.0155, <http://rsta.royalsocietypublishing.org/content/373/2041/20140155.full.pdf>.
- [3] C. H. K. Chen, *Journal of Plasma Physics* **82**, 535820602 (2016), arXiv:1611.03386 [physics.plasm-ph].
- [4] J. J. Podesta, D. A. Roberts, and M. L. Goldstein, *Astrophys. J.* **664**, 543 (2007).
- [5] C. Salem, A. Mangeney, S. D. Bale, and P. Veltri, *Astrophys. J.* **702**, 537 (2009).
- [6] D. A. Roberts, *Journal of Geophysical Research (Space Physics)* **115**, A12101 (2010).
- [7] R. T. Wicks, T. S. Horbury, C. H. K. Chen, and A. A. Schekochihin, *Physical Review Letters* **106**, 045001 (2011), arXiv:1009.2427 [physics.plasm-ph].
- [8] J. A. Tessein, C. W. Smith, B. T. MacBride, W. H. Matthaeus, M. A. Forman, and J. E. Borovsky, *Astrophys. J.* **692**, 684 (2009).
- [9] C. H. K. Chen, S. D. Bale, C. Salem, and F. S. Mozer, *Astrophys. J. Let.* **737**, L41 (2011), arXiv:1105.2390 [physics.space-ph].
- [10] R. J. Leamon, C. W. Smith, N. F. Ness, W. H. Matthaeus, and H. K. Wong, *J. Geophys. Res.* **103**, 4775 (1998).
- [11] C. W. Smith, K. Hamilton, B. J. Vasquez, and R. J. Leamon, *Astrophys. J. Let.* **645**, L85 (2006).
- [12] F. Sahraoui, M. L. Goldstein, G. Belmont, P. Canu, and L. Rezeau, *Physical Review Letters* **105**, 131101 (2010).
- [13] O. Alexandrova, J. Saur, C. Lacombe, A. Mangeney, J. Mitchell, S. J. Schwartz, and P. Robert, *Physical Review Letters* **103**, 165003 (2009), arXiv:0906.3236 [physics.plasm-ph].
- [14] O. Alexandrova, C. Lacombe, A. Mangeney, R. Grappin, and M. Maksimovic, *Astrophys. J.* **760**, 121 (2012), arXiv:1212.0412 [astro-ph.SR].
- [15] J. Šafránková, Z. Němeček, F. Němec, L. Přech, C. H. K. Chen, and G. N. Zastenker, *Astrophys. J.* **825**, 121 (2016).

- [16] S. D. Bale, P. J. Kellogg, F. S. Mozer, T. S. Horbury, and H. Reme, *Phys. Rev. Lett.* **94**, 215002 (2005).
- [17] P. J. Kellogg, S. D. Bale, F. S. Mozer, T. S. Horbury, and H. Reme, *Astrophys. J.* **645**, 704 (2006), physics/0602179.
- [18] J. E. Stawarz, S. Eriksson, F. D. Wilder, R. E. Ergun, S. J. Schwartz, A. Pouquet, J. L. Burch, B. L. Giles, Y. Khotyaintsev, O. Le Contel, P.-A. Lindqvist, W. Magnes, C. J. Pollock, C. T. Russell, R. J. Strangeway, R. B. Torbert, L. A. Avanov, J. C. Dorelli, J. P. Eastwood, D. J. Gershman, K. A. Goodrich, D. M. Malaspina, G. T. Marklund, L. Mirioni, and A. P. Sturmer, *Journal of Geophysical Research (Space Physics)* **121**, 11 (2016).
- [19] L. Matteini, O. Alexandrova, C. H. K. Chen, and C. Lacombe, *MNRAS* **466**, 945 (2017).
- [20] L. Franci, S. Landi, L. Matteini, A. Verdini, and P. Hellinger, *Astrophys. J.* **812**, 21 (2015), arXiv:1506.05999 [astro-ph.SR].
- [21] C. H. K. Chen, L. Leung, S. Boldyrev, B. A. Maruca, and S. D. Bale, *Geophys. Res. Lett.* **41**, 8081 (2014).
- [22] R. Bruno and L. Trenchi, *Astrophys. J. Let.* **787**, L24 (2014), arXiv:1404.2191 [astro-ph.SR].
- [23] L. Franci, S. Landi, L. Matteini, A. Verdini, and P. Hellinger, *Astrophys. J.* **833**, 91 (2016), arXiv:1610.05158 [physics.space-ph].
- [24] C. S. Salem, G. G. Howes, D. Sundkvist, S. D. Bale, C. C. Chaston, C. H. K. Chen, and F. S. Mozer, *Astrophys. J. Let.* **745**, L9 (2012).
- [25] K. H. Kiyani, S. C. Chapman, F. Sahraoui, B. Hnat, O. Fauvarque, and Y. V. Khotyaintsev, *Astrophys. J.* **763**, 10 (2013), arXiv:1008.0525 [physics.space-ph].
- [26] J. J. Podesta and J. M. TenBarge, *Journal of Geophysical Research (Space Physics)* **117**, A10106 (2012).
- [27] J. Šafránková, Z. Němeček, F. Němec, L. Přech, A. Pitňa, C. H. K. Chen, and G. N. Zastenker, *Astrophys. J.* **803**, 107 (2015).
- [28] C. H. K. Chen, S. Boldyrev, Q. Xia, and J. C. Perez, *Physical Review Letters* **110**, 225002 (2013), arXiv:1305.2950 [physics.space-ph].
- [29] S. Oughton, E. R. Priest, and W. H. Matthaeus, *Journal of Fluid Mechanics* **280**, 95 (1994).
- [30] J. Cho and E. T. Vishniac, *Astrophys. J.* **539**, 273 (2000), astro-ph/0003403.
- [31] J. Maron and P. Goldreich, *Astrophys. J.* **554**, 1175 (2001), astro-ph/0012491.
- [32] J. Cho and A. Lazarian, *Physical Review Letters* **88**, 245001 (2002), astro-ph/0205282.
- [33] W.-C. Müller and R. Grappin, *Physical Review Letters* **95**, 114502 (2005), physics/0509019.
- [34] J. Mason, F. Cattaneo, and S. Boldyrev, *Phys. Rev. E* **77**, 036403 (2008), arXiv:0706.2003.
- [35] A. Beresnyak and A. Lazarian, *Astrophys. J.* **702**, 460 (2009), arXiv:0904.2574 [astro-ph.SR].
- [36] R. Grappin and W.-C. Müller, *Phys. Rev. E* **82**, 026406 (2010), arXiv:1008.0727 [physics.plasm-ph].
- [37] E. Lee, M. E. Brachet, A. Pouquet, P. D. Mininni, and D. Rosenberg, *Phys. Rev. E* **81**, 016318 (2010), arXiv:0906.2506 [physics.flu-dyn].
- [38] J. C. Perez and S. Boldyrev, *Physical Review Letters* **102**, 025003 (2009), arXiv:0807.2635.
- [39] S. Boldyrev, J. C. Perez, J. E. Borovsky, and J. J. Podesta, *Astrophys. J. Let.* **741**, L19 (2011), arXiv:1106.0700 [astro-ph.GA].
- [40] C. H. K. Chen, A. Mallet, T. A. Yousef, A. A. Schekochihin, and T. S. Horbury, *MNRAS* **415**, 3219 (2011), arXiv:1009.0662 [physics.space-ph].
- [41] Y. Dong, A. Verdini, and R. Grappin, *Astrophys. J.* **793**, 118 (2014), arXiv:1409.0018 [astro-ph.SR].
- [42] A. Verdini and R. Grappin, *Astrophys. J. Let.* **808**, L34 (2015), arXiv:1506.03450 [astro-ph.SR].
- [43] A. Verdini and R. Grappin, *Astrophys. J.* **831**, 179 (2016), arXiv:1609.09094 [astro-ph.SR].
- [44] A. Verdini, R. Grappin, P. Hellinger, S. Landi, and W. C. Müller, *Astrophys. J.* **804**, 119 (2015), arXiv:1502.04705 [astro-ph.SR].
- [45] P. Goldreich and S. Sridhar, *Astrophys. J.* **438**, 763 (1995).
- [46] P. Goldreich and S. Sridhar, *Astrophys. J.* **485**, 680 (1997), astro-ph/9612243.
- [47] S. Galtier, S. V. Nazarenko, A. C. Newell, and A. Pouquet, *Journal of Plasma Physics* **63**, 447 (2000), astro-ph/0008148.
- [48] J. Cho, A. Lazarian, and E. T. Vishniac, *Astrophys. J. Let.* **566**, L49 (2002), astro-ph/0112195.
- [49] J. W. Bieber, W. Wanner, and W. H. Matthaeus, *J. Geophys. Res. (Space Phys.)* **101**, 2511 (1996).
- [50] T. S. Horbury, M. Forman, and S. Oughton, *Physical Review Letters* **101**, 175005 (2008), arXiv:0807.3713 [physics.plasm-ph].
- [51] J. J. Podesta, *Astrophys. J.* **698**, 986 (2009), arXiv:0901.4940 [astro-ph.EP].
- [52] A. Verdini, R. Grappin, O. Alexandrova, and S. Lion, *Astrophys. J.* **853**, 85 (2018), arXiv:1802.09837 [astro-ph.SR].
- [53] A. Verdini, R. Grappin, O. Alexandrova, L. Franci, S. Landi, L. Matteini, and E. Papini, arXiv e-prints, arXiv:1904.04118 (2019), arXiv:1904.04118 [astro-ph.SR].
- [54] A. A. Schekochihin, S. C. Cowley, W. Dorland, G. W. Hammett, G. G. Howes, E. Quataert, and T. Tatsuno, *Astrophys. J. Supl. Series* **182**, 310 (2009), arXiv:0704.0044.
- [55] D. Biskamp, E. Schwarz, and J. F. Drake, *Physical Review Letters* **76**, 1264 (1996).
- [56] D. Biskamp, E. Schwarz, A. Zeiler, A. Celani, and J. F. Drake, *Physics of Plasmas* **6**, 751 (1999).
- [57] C. S. Ng, A. Bhattacharjee, K. Germaschewski, and S. Galtier, *Physics of Plasmas* **10**, 1954 (2003).
- [58] J. Cho and A. Lazarian, *Astrophys. J. Let.* **615**, L41 (2004), astro-ph/0406595.
- [59] D. Shaikh, *MNRAS* **395**, 2292 (2009), arXiv:0902.4420 [physics.space-ph].
- [60] D. Shaikh and P. K. Shukla, *Physical Review Letters* **102**, 045004 (2009).
- [61] G. G. Howes, W. Dorland, S. C. Cowley, G. W. Hammett, E. Quataert, A. A. Schekochihin, and T. Tatsuno, *Physical Review Letters* **100**, 065004 (2008), arXiv:0711.4355.
- [62] G. G. Howes, J. M. TenBarge, W. Dorland, E. Quataert, A. A. Schekochihin, R. Numata, and T. Tatsuno, *Physical Review Letters* **107**, 035004 (2011), arXiv:1104.0877 [astro-ph.SR].
- [63] J. M. TenBarge and G. G. Howes, *Physics of Plasmas* **19**, 055901 (2012), arXiv:1201.0056 [physics.plasm-ph].
- [64] T. Passot and P. L. Sulem, *Astrophys. J. Let.* **812**, L37 (2015), arXiv:1509.02839 [physics.plasm-ph].
- [65] T. Passot, P. Henri, D. Laveder, and P.-L. Sulem, *European Physical Journal D* **68**, 207 (2014).
- [66] P. L. Sulem, T. Passot, D. Laveder, and D. Borgogno, *Astrophys. J.* **818**, 66 (2016), arXiv:1511.01256 [astro-ph.SR].
- [67] E. Camporeale and D. Burgess, *Astrophys. J.* **730**, 114 (2011), arXiv:1101.6032 [physics.space-ph].
- [68] S. P. Gary, O. Chang, and J. Wang, *Astrophys. J.* **755**, 142 (2012).
- [69] P. Hellinger, A. Verdini, S. Landi, L. Franci, and L. Matteini, *Astrophys. J. Let.* **857**, L19 (2018), arXiv:1803.09572

- [physics.space-ph].
- [70] E. Papini, L. Franci, S. Landi, A. Verdini, L. Matteini, and P. Hellinger, *Astrophys. J.* **870**, 52 (2019), arXiv:1810.02210 [physics.plasm-ph].
- [71] P. Dmitruk and W. H. Matthaeus, *Physics of Plasmas* **13**, 042307 (2006).
- [72] S. Servidio, F. Valentini, D. Perrone, A. Greco, F. Califano, W. H. Matthaeus, and P. Veltri, *Journal of Plasma Physics* **81**, 325810107 (2015).
- [73] M. Wan, W. H. Matthaeus, V. Roytershteyn, H. Karimabadi, T. Parashar, P. Wu, and M. Shay, *Physical Review Letters* **114**, 175002 (2015).
- [74] S. Boldyrev and J. C. Perez, *Astrophys. J. Let.* **758**, L44 (2012), arXiv:1204.5809 [astro-ph.SR].
- [75] S. Boldyrev, K. Horaites, Q. Xia, and J. C. Perez, *Astrophys. J.* **777**, 41 (2013).
- [76] R. Meyrand and S. Galtier, *Physical Review Letters* **111**, 264501 (2013).
- [77] S. S. Cerri, S. Servidio, and F. Califano, *Astrophys. J. Let.* **846**, L18 (2017), arXiv:1707.08429 [physics.plasm-ph].
- [78] L. Franci, S. Landi, A. Verdini, L. Matteini, and P. Hellinger, *Astrophys. J.* **853**, 26 (2018), arXiv:1711.02664 [physics.space-ph].
- [79] L. Arzamasskiy, M. W. Kunz, B. D. G. Chandran, and E. Quataert, arXiv e-prints (2019), arXiv:1901.11028 [astro-ph.HE].
- [80] A. Mallet, A. A. Schekochihin, and B. D. G. Chandran, *Journal of Plasma Physics* **83**, 905830609 (2017), arXiv:1707.05907 [physics.plasm-ph].
- [81] N. F. Loureiro and S. Boldyrev, *Physical Review Letters* **118**, 245101 (2017).
- [82] S. Boldyrev and N. F. Loureiro, *Astrophys. J.* **844**, 125 (2017), arXiv:1706.07139 [physics.plasm-ph].
- [83] N. F. Loureiro and S. Boldyrev, *Astrophys. J.* **850**, 182 (2017), arXiv:1707.05899 [physics.plasm-ph].
- [84] L. Franci, S. S. Cerri, F. Califano, S. Landi, E. Papini, A. Verdini, L. Matteini, F. Jenko, and P. Hellinger, *Astrophys. J. Let.* **850**, L16 (2017), arXiv:1707.06548 [physics.space-ph].
- [85] S. S. Cerri and F. Califano, *New Journal of Physics* **19**, 025007 (2017).
- [86] L. Franci, P. Hellinger, M. Guarrasi, C. H. K. Chen, E. Papini, A. Verdini, L. Matteini, and S. Landi, *Journal of Physics: Conference Series* **1031**, 012002 (2018).
- [87] A. P. Matthews, *Journal of Computational Physics* **112**, 102 (1994).
- [88] J. Cho and A. Lazarian, *Astrophys. J.* **701**, 236 (2009), arXiv:0904.0661 [astro-ph.EP].
- [89] E. Falcon, S. Fauve, and C. Laroche, *Physical Review Letters* **98**, 154501 (2007), physics/0612254.
- [90] W. H. Matthaeus, S. Oughton, S. Ghosh, and M. Hossain, *Physical Review Letters* **81**, 2056 (1998).
- [91] S. Oughton, W. H. Matthaeus, and S. Ghosh, *Physics of Plasmas* **5**, 4235 (1998).
- [92] U. Frisch, *Turbulence. The legacy of A. N. Kolmogorov.*, 1st ed. (Cambridge University Press, 1995).
- [93] L. Franci, A. Verdini, L. Matteini, S. Landi, and P. Hellinger, *Astrophys. J. Let.* **804**, L39 (2015), arXiv:1503.05457 [astro-ph.SR].
- [94] S. S. Cerri, F. Califano, F. Jenko, D. Told, and F. Rincon, *Astrophys. J. Let.* **822**, L12 (2016), arXiv:1604.07674 [physics.plasm-ph].
- [95] N. F. Loureiro, A. A. Schekochihin, and S. C. Cowley, *Physics of Plasmas* **14**, 100703 (2007), arXiv:astro-ph/0703631.
- [96] A. Bhattacharjee, Y.-M. Huang, H. Yang, and B. Rogers, *Physics of Plasmas* **16**, 112102 (2009), arXiv:0906.5599 [physics.plasm-ph].
- [97] F. Pucci and M. Velli, *Astrophys. J.* **780**, L19 (2014).
- [98] S. Landi, L. Del Zanna, E. Papini, F. Pucci, and M. Velli, *Astrophys. J.* **806**, 131 (2015).
- [99] A. Tenerani, M. Velli, A. F. Rappazzo, and F. Pucci, *Astrophys. J. Let.* **813**, L32 (2015), arXiv:1506.08921 [physics.plasm-ph].
- [100] D. Del Sarto, F. Pucci, A. Tenerani, and M. Velli, *Journal of Geophysical Research (Space Physics)* **121**, 1857 (2016), arXiv:1511.00035 [physics.plasm-ph].
- [101] F. Pucci, M. Velli, and A. Tenerani, ArXiv e-prints (2017), arXiv:1704.08793 [astro-ph.SR].
- [102] D. Del Sarto and M. Ottaviani, *Physics of Plasmas* **24**, 012102 (2017), arXiv:1603.00276 [physics.plasm-ph].
- [103] A. Mallet, A. A. Schekochihin, and B. D. G. Chandran, *MNRAS* **468**, 4862 (2017), arXiv:1612.07604 [astro-ph.SR].
- [104] C. Dong, L. Wang, Y.-M. Huang, L. Comisso, and A. Bhattacharjee, *Physical Review Letters* **121**, 165101 (2018), arXiv:1804.07361 [physics.plasm-ph].
- [105] R. Bruno, L. Trenchi, and D. Telsoni, *Astrophys. J. Let.* **793**, L15 (2014), arXiv:1408.4595 [astro-ph.SR].
- [106] C. H. K. Chen, T. S. Horbury, A. A. Schekochihin, R. T. Wicks, O. Alexandrova, and J. Mitchell, *Physical Review Letters* **104**, 255002 (2010), arXiv:1002.2539 [physics.space-ph].
- [107] W. H. Matthaeus, R. Bandyopadhyay, M. R. Brown, J. Borovsky, V. Carbone, D. Caprioli, A. Chasapis, R. Chhiber, S. Dasso, P. Dmitruk, L. Del Zanna, P. A. Dmitruk, L. Franci, S. P. Gary, M. L. Goldstein, D. Gomez, A. Greco, T. S. Horbury, H. Ji, J. C. Kasper, K. G. Klein, S. Landi, H. Li, F. Malara, B. A. Maruca, P. Mininni, S. Oughton, E. Papini, T. N. Parashar, A. Petrosyan, A. Pouquet, A. Retino, O. Roberts, D. Ruffolo, S. Servidio, H. Spence, C. W. Smith, J. E. Stawarz, J. TenBarge, B. J. Vasquez1, A. Whittvads, F. Valentini, M. Velli, A. Verdini, D. Verscharen, P. Whittlesey, R. Wicks, R. Bruno, and G. Zimbardo, arXiv e-prints (2019), arXiv:1903.06890 [physics.space-ph].
- [108] K. G. Klein, O. Alexandrova, J. Bookbinder, D. Caprioli, A. W. Case, B. D. G. Chandran, L. J. Chen, T. Horbury, L. Jian, J. C. Kasper, O. Le Contel, B. A. Maruca, W. Matthaeus, A. Retino, O. Roberts, A. Schekochihin, R. Skoug, C. Smith, J. Steinberg, H. Spence, B. Vasquez, J. M. TenBarge, D. Verscharen, and P. Whittlesey, arXiv e-prints (2019), arXiv:1903.05740 [physics.plasm-ph].
- [109] J. M. TenBarge, O. Alexandrova, S. Boldyrev, F. Califano, S. S. Cerri, C. H. K. Chen, G. G. Howes, T. Horbury, P. A. Isenberg, H. Ji, K. G. Klein, C. Krafft, M. Kunz, N. F. Loureiro, A. Mallet, B. A. Maruca, W. H. Matthaeus, R. Meyrand, E. Quataert, J. C. Perez, O. W. Roberts, F. Sahnou, C. S. Salem, A. A. Schekochihin, H. Spence, J. Squire, D. Told, D. Verscharen, and R. T. Wicks, arXiv e-prints (2019), arXiv:1903.05710 [physics.space-ph].